

# Interpretable Video based Stress Detection with Self-Refine Chain Reasoning

Yi Dai, Yang Ding, Lei Cao, Kaisheng Zeng, Junrui Tian, Zexi Lin, Ling Feng

Department of Computer Science and Technology, Tsinghua University, Beijing, China

Faculty of Psychology, Beijing Normal University, Beijing, China

{dai-y21, dingy20, zks18, tjr21, linzx22}@mails.tsinghua.edu.cn, fengling@mail.tsinghua.edu.cn, caolei@bnu.edu.cn

**Abstract**—Stress detection is critical for mental and physical well-being, yet traditional methods such as self-reports and physiological sensors face limitations in efficiency and scalability. Video-based stress detection, leveraging visual cues learned from an annotated video database, offers a non-invasive, cost-effective alternative. However, most models function as black boxes, lacking transparency in their decision-making process, which hinders their trustworthiness. To address this, we propose an interpretable video-based stress detection model that incorporates Chain-of-Thought (CoT) reasoning of large foundation models. Our model follows a structured reasoning chain “*Describe*→*Assess*→*Highlight*”, mimicking the decision process of psychology experts. To further enhance model reliability, we integrate a self-refinement mechanism that allows the model to reflect on and improve its predictions using Direct Preference Optimization (DPO) to ensure accuracy and faithfulness. Experimental results on two video-based stress detection datasets demonstrate that our approach outperforms state-of-the-art models in both accuracy and interpretability.

**Index Terms**—Stress detection, interpretable, Chain-of-Thought (CoT) reasoning, and self-refinement.

## I. INTRODUCTION

Stress has become a significant concern in modern society with far-reaching impacts on both mental and physical health. As such, timely and accurate stress detection is crucial for performing preventive health measures and interventions. Traditional stress detection methods based on self-reports and physiological sensors, while effective, may suffer from practical drawbacks such as being intrusive and laborious, making them limited in efficiency and scalability. With video becoming an integral part of social media and surveillance systems being widely applied, detecting stress from videos based on handcrafted or deeply learned features has attracted research attention due to its non-invasiveness, low-cost, and mass-reaching advantages. By learning to analyze such visual cues from video footage within an annotated video database, stress can be detected without physical contact in an end-to-end manner [1].

However, most existing stress detection models operate as “black boxes”, providing predictions without any insight into the reasoning behind their decisions. This lack of interpretability limits the trustworthiness and applicability of these models. For sensitive domains such as stress detection, understanding the basis of a decision is as important as the decision itself [2]. The only way to explain a black-box model is to employ a post-hoc explainer as a surrogate model to explain the model decision [3]. For each sample, the surrogate model requires

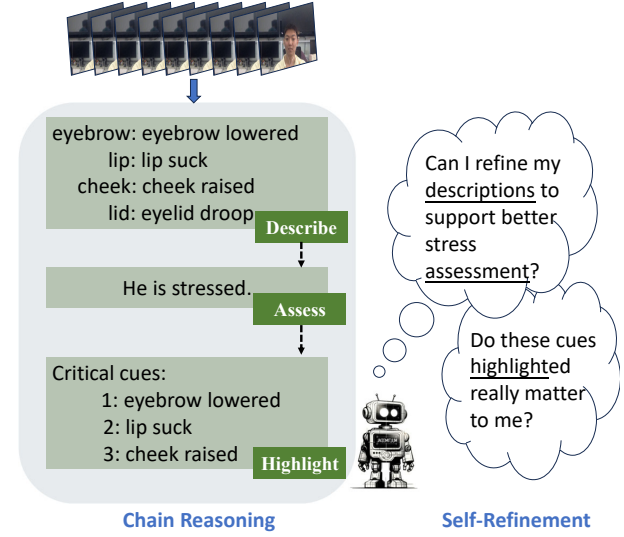


Fig. 1: A large foundation model could perform video based stress detection with chain reasoning to generate rationales along with predictions. Meanwhile, it could reflect on and refine its generations to enhance interpretability.

making perturbations on the input and acquiring outputs from the original model, which is usually computational prohibitive.

With the advent of large foundation models trained on massive amounts of diverse datasets and excelling in natural language and video processing, performance of stress detection via large foundation models could be remarkably boosted by their world knowledge [4]. Moreover, Chain-of-Thought (CoT) [5], a promising technique emerging most recently, exploits commonsense knowledge and reasoning ability of large foundation models to remarkably enhance both performance and interpretability by guiding them to generate intermediate reasoning chains to infer the answer, making the model decision process more transparent and human understandable.

The aim of the study is to explore the use of large foundation models coupled with CoT reasoning for interpretable video based stress detection. Specifically, we transform the end-to-end prediction task into a step-by-step reasoning problem to emulate the thought process of a psychology expert [6]: the proposed model first analyzes and **describes** user’s facial expressions in the video clips, then **assesses** user’s stress level, and finally

**highlights** the key visual cues that influenced its judgment as rationale. After acquiring the knowledge to identify facial expressions via instruction tuning with expert annotation, the model will follow such a “*Describe→Assess→Highlight*” reasoning chain to elicit stress level prediction and rationales.

To address two possible types of errors introduced by the CoT scheme [7], namely, (1) factual errors: the generated visual cues and the prediction result could be inaccurate due to insufficient professional expertise compared with human experts, and (2) hallucination errors: although Chain-of-Thought resemble human reasoning on a surface level, the concluded key visual cue may not faithfully reflect the true factors influencing the model’s decisions, making the provided rationale untrustworthy, we train the model to reflect on its errors and generate refined descriptions, assessments, and highlighted visual cues, as illustrated in Figure 1. Meanwhile, to avoid unfaithful generation, we design a self-verification scheme to check if the model faithfully describes the facial expressions of the user, and the highlighted visual cue significantly influences the model decision. The model finally learns from refined generations through Direct Preference Optimization (DPO) [8]. In this way, the reasoning chain and self-refinement process strengthen not only the accuracy of model detection performance but also the model interpretability.

The key contributions of the paper can be summarized as follows.

- We propose a “*Describe→Assess→Highlight*” reasoning chain, which formally transforms video-based stress detection into a step-by-step reasoning process, enabling the model to perform stress detection and provide highlighted visual cues as rationale.
- We design a self-refine learning scheme, in which large foundation models can reflect on its mistakes and unfaithful outputs, learning to refine its reasoning results during the training process. It makes the model rationale faithful without requiring additional computation overhead during deployment.

Our extensive experimentation on two video datasets UVSD and RSL demonstrates that (1) our model consistently outperforms the state-of-the-art, achieving 95.81% and 90.94% of accuracy on UVSD and RSL, respectively; (2) self-refinement helps improve the performance by 2.25% and 2.15% of accuracy on UVSD and RSL, respectively; (3) CoT enables to increase the performance by 4.07% and 3.96% of accuracy on UVSD and RSL, respectively; (4) disturbing the Top-1 segment highlighted by our method results in the accuracy drop by 11.96% on UVSD and 14.70% on RSL, respectively, showcasing the faithfulness of the rationale generated by our method; and (5) the proposed method could generate a rationale within 3.4 seconds, which is 63 times faster than the most efficient baseline explainer SOBOL with 216.3 seconds.

To our knowledge, this is the first attempt in the literature that integrates Chain-of-Thought reasoning of large foundation models with self-refinement into the stress detection task to gain interpretability and detection performance. It shows an effective way to utilize large foundations models coupled with

Chain-of-Thought reasoning and self-refinement learning to handle a large scope of tasks in different fields.

## II. RELATED WORK

### A. Video-based Stress Detection

With the widespread use of social media and the increasing prevalence of surveillance devices, video-based stress detection has garnered significant attention in recent years, offering notable advantages such as low cost and non-invasive detection. A line of studies in video-based stress detection focus on the model architecture extracting information from the visual input. Jeon et al. [9] combines spatial and temporal attention for face image encoding, which enables the model to focus on frames highly correlated with stress and the regions on a single frame that are highly correlated with stress. Zhang et al. [10] combines the dynamics of body action when encoding images for stress detection, introducing a two-level stress detection network named TSDNET. To control computational overhead, TSDNET employs facial emotion recognition to obtain the most expressive and most expressionless facial images in the video to generate emotions representations. Meanwhile, a line of studies exploit the correlation between emotions and stress, as stress is sensitive to negative emotions such as anger, fear and sadness [11, 12]. Zhang et al. [11] first detects the expressed emotion from each video frame, then predicts whether the subject is stressed based on the ratio of negative emotions within the video. In prior psychological studies, facial expressions can be decomposed into a group of units, in which certain co-occurrence of units can reveal states of inner feeling [13]. During psychological state diagnosis, experts first detect facial action units (AUs) from facial expressions and then make decision referring to the states of AUs [6]. AUs are also observed to be valuable in predicting stress, in which the stress states can be predicted using the occurrence of AUs [14, 15]. Inspired by the diagnosis process of experts, we guide the model to perform facial action (AU) detection first, and then predict the stress states according to detected AUs and the original video.

### B. Explanation for “Black-box” Models

The only method to explain the decision of a “black-box” model is to employ post-hoc explainers, which intuitively observes how the model’s predictions change as the inputs vary [16]. Local interpretable model-agnostic explanations (LIME) [17] and Shapley Additive exPlanations (SHAP) [18] are the most widely used post-hoc explainers, which remove multiple features at the same time to observe the assign attribution scores to input features. Concretely, given an instance, LIME builds an interpretable linear model to approximate the behavior of the initially trained model towards the input instance. It generates a new dataset of perturbed instances based on the input, and obtains corresponding predictions from the initially trained model as labels. Subsequently, a linear model is trained on the perturbed set of instances, and its linear coefficients represent the importance of each token in the prediction. In a similar manner, SHAP uses a

game theory to explain model’s predictions. Specifically, it computes the Shapley values by evaluating the initial model under different combinations of input features and calculating the average difference in the model output. Nevertheless, they are computationally expensive to compute the importance of each input part [19]. For example, in Python `lime` package, the default number of perturbations on the original input is set to 5000 times<sup>1</sup>. Hence, strategies to make the explanation process more efficient are envisaged, especially for large foundation models that require more computation. In this study, we capitalize on the Chain-of-Thought reasoning ability of large foundation models, and employ self-refining to make their decision process more interpretable.

### C. Chain-of-Thought Reasoning

Chain-of-Thought (CoT) has gained significant attention, in which a foundation model is prompted to generate a series of short sentences that mimic the reasoning steps a person might employ in solving a task [5]. Following this line, a gamut of ways have been explored to enhance the performance of CoT reasoning [20, 21, 22, 23, 24] by diversifying the input prompts and reasoning form of COT. For instance, Li et al. [22] guides the foundation model to recall relevant memory to help itself reason and answer questions. Meanwhile, CoT reasoning has been observed efficient across various domains [25, 26, 27, 28]. Lee et al. [28] employs a step-by-step prompt to guide the foundation model to provide consumer health support. Nachane et al. [26] designs a medical prompt template to guide the foundation model to answer open-domain medical questions.

Despite its effectiveness, CoT reasoning is not without challenges. One of the primary concerns is that CoT may not faithfully reflect the model’s true reasoning process [29], i.e., standard CoT does not provide interpretability of how the model predicts the answer. In addition, errors can propagate throughout the chain of reasoning, requiring the quality of each reasoning step. If the model makes an incorrect inference early in the process, subsequent steps may build on that faulty assumption, leading to compounding errors and inaccurate conclusions. In this study, we develop a Chain-of-Thought reasoning scheme that learns to refine its unfaithful and incorrect generation throughout the training process.

## III. METHODOLOGY

### A. Problem Setup and Overall Framework

Given a video  $\mathcal{V}$  of a subject from dataset  $D$ , we aim to employ a generative vision-language foundation model  $F$  to (1) detect whether the subject is stressed, and (2) provide rationale for the detection result. Inspired by the reasoning process of psychologists [6], we design a Chain-of-Thought reasoning scheme for our model  $F$  following three steps. **(1) Describe:** Given video  $\mathcal{V}$ , model  $F$  recognizes facial expressions  $\mathcal{E}$  of the subject guided by instruction  $\mathcal{I}_1$ , consisting of a set of linguistic descriptions about different facial movements. **(2) Assess:** Given a new instruction  $\mathcal{I}_2$ ,  $F$  assesses whether the

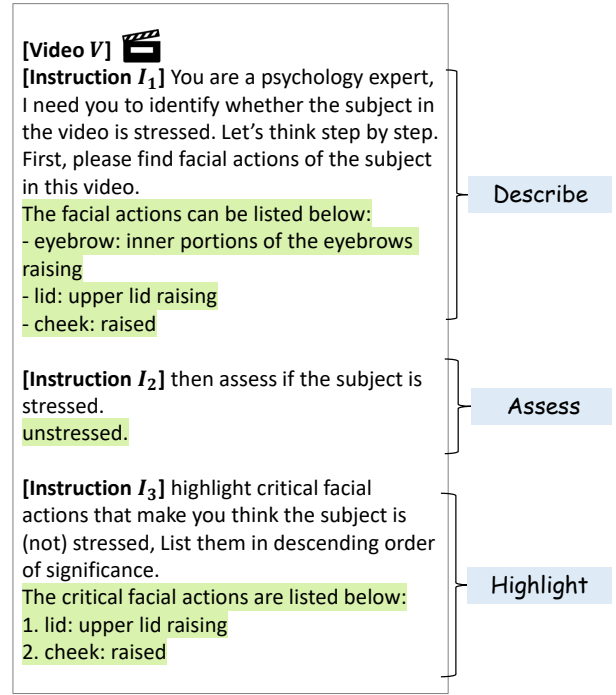


Fig. 2: Illustration of our proposed Reasoning Chain, where the text marked in green is generated by the model  $F$ . It includes three main steps: (1) Describe the facial expressions from the video, (2) Assess the stress level based on the original video and generated expressions, and (3) Highlight the critical facial expressions that influenced the stress assessment.

subject is under stress with  $\mathcal{V}$  and  $\mathcal{E}$ , classifying it as  $\mathcal{A} \in \{\text{Stressed, Unstressed}\}$ . **(3) Highlight:** model  $F$  finally provides critical facial expressions  $\mathcal{R}$  as rationale for its decision  $\mathcal{A}$  with instruction  $\mathcal{I}_3$ . The input and outputs of the model are illustrated in Figure 2, which consists of three steps.

The entire reasoning process could be formulated as:

$$p_F(\mathcal{R}, \mathcal{A}, \mathcal{E} \mid \mathcal{V}) = p_F(\mathcal{R} \mid \mathcal{A}, \mathcal{E}, \mathcal{V}, \mathcal{I}_3) \cdot p_F(\mathcal{A} \mid \mathcal{E}, \mathcal{V}, \mathcal{I}_2) \cdot p_F(\mathcal{E} \mid \mathcal{V}, \mathcal{I}_1). \quad (1)$$

### B. Learn to Describe Facial Actions

Inspired by the reasoning process of psychologists [6], we capablize our model to recognize and report facial expressions systematically. Specifically, we perform instruction tuning with expert-annotated facial action unit (AU) data. The facial expressions of the subject in each video are decomposed into actions appearing on different facial regions, named Action Units (AUs) [30]. We construct a facial action description dataset  $D'$  with instruction answer pairs  $\langle \mathcal{V}, \mathcal{E} \rangle$  to equip the model  $F$  with the ability to detect facial actions. For each video  $\mathcal{V}$ , we transform the target action unit label into natural linguistic description  $\mathcal{E}$ . The model  $F$  then learns to generate facial expression description, given the question answer pairs, i.e., only learning the ‘‘Describe’’ step.

<sup>1</sup><https://lime-ml.readthedocs.io/en/latest/>

$$\mathcal{L}_{desc} = -\mathbb{E}_{(\mathcal{V}, \mathcal{E}) \sim D'} [p_F(\mathcal{E} \mid \mathcal{V}, \mathcal{I}_1)]. \quad (2)$$

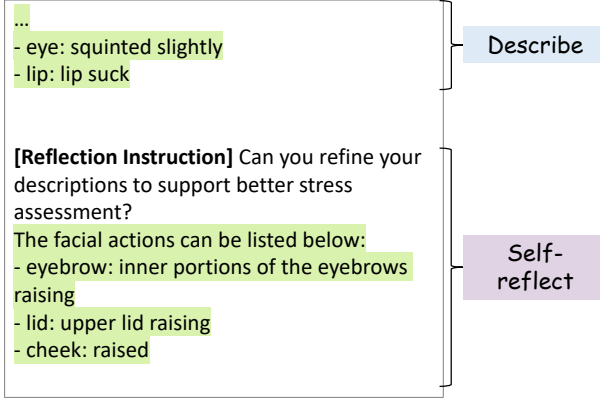


Fig. 3: Illustration of Self-reflection process on facial description  $\mathcal{E}$ , where model  $F$  is instructed to reflect on its descriptions and generate a new one.

### C. Detect Stress with Facial Action Descriptions

For each video sample  $\mathcal{V}$  from the training set of  $D$ ,  $F$  is first instructed by  $I_1$  to generate facial action description  $\mathcal{E}$  from  $\mathcal{V}$ .

**Self-refinement for Description.** “*Could I refine my descriptions to support better stress Assessment?*” Since the stress detection result  $\mathcal{A}$  and rationale  $\mathcal{R}$  are generated as the reasoning outcome of  $\mathcal{E}$ , the detection accuracy can largely benefit from high-quality facial descriptions  $\mathcal{E}$ . Conversely, improper descriptions could result in compounding errors. To enhance the quality of  $\mathcal{E}$ , we introduce “Self-reflection” instruction that guides the model to reflect on its previous descriptions, predict the stress level based on the ground truth, and generate a new description  $\mathcal{E}'$ . The reflection instruction prompt is illustrated in Figure 3.

We compare the quality of  $\mathcal{E}$  and the updated description  $\mathcal{E}'$  along two dimensions, i.e., helpfulness and faithfulness. (1) **helpfulness** evaluates whether model  $F$  can accurately predict the stress level  $\mathcal{A}$  with  $\mathcal{E}$ , i.e.,  $p_F(\mathcal{A}|\mathcal{V}, \mathcal{E}, \mathcal{I}_2)$ . We prompt the model to answer  $\mathcal{I}_2$  based on  $\mathcal{E}$  and  $\mathcal{E}'$   $K$  times with different random seeds, and obtain accuracy scores  $h$  and  $h'$ . The helpfulness of  $\mathcal{E}'$  is better, only if  $h' \geq h$ . (2) **faithfulness** is evaluated with a self-verification process whether description honestly describes the original video  $\mathcal{V}$ . Specifically, besides the current video sample  $\mathcal{V}$ , we also randomly select 3 video samples from other subjects as negative samples, and prompt the model to select the correct sample that  $\mathcal{E}$  or  $\mathcal{E}'$  describes out of the 4 videos, as illustrated in Figure 4. Note that the self-verification is started in another dialogue session, in which the model cannot “cheat” by reading dialogue history.

After repeating the multi-choice selection  $K$  times, accuracy score  $f'$  and  $f$  can be obtained for  $\mathcal{E}'$  and  $\mathcal{E}$ , indicating their faithfulness. If  $f' \geq f$  and  $h' \geq h$ , we replace  $\mathcal{E}$  with  $\mathcal{E}'$ . We repeat the self-reflection process until the description  $\mathcal{E}$  cannot be replaced with new descriptions. We record the original description  $\mathcal{E}_o$  and let model  $F$  learn to understand  $\mathcal{E}$  is superior

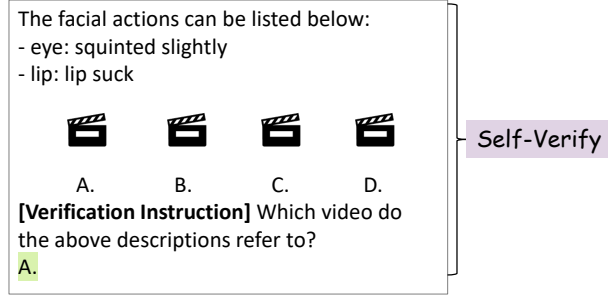


Fig. 4: Illustration of Self-verification process on facial description  $\mathcal{E}$ , where model  $F$  is instructed to select a video that  $\mathcal{E}$  describes without any context (i.e., dialogue history).

to  $\mathcal{E}_o$  via Direct Preference Optimization (DPO):

$$\mathcal{L}_{refine\mathcal{E}} = -\mathbb{E}_{\mathcal{V} \sim D} [\log \sigma(\beta \log \frac{p_F(\mathcal{E}|\mathcal{V}, \mathcal{I}_1)}{p_{ref}(\mathcal{E}|\mathcal{V}, \mathcal{I}_1)} - \beta \log \frac{p_F(\mathcal{E}_o|\mathcal{V}, \mathcal{I}_1)}{p_{ref}(\mathcal{E}_o|\mathcal{V}, \mathcal{I}_1)})], \quad (3)$$

where  $ref$  denotes the initial parameter of model  $F$  before training to avoid over-optimization,  $\sigma$  denotes Sigmoid function, and  $\beta$  is scalar hyper-parameter.

With video  $\mathcal{V}$  and updated description  $\mathcal{E}$ , model  $F$  is guided by instruction  $\mathcal{I}_2$  to assess stress level  $\mathcal{A}$  of the subject:

$$\mathcal{L}_{assess} = -\mathbb{E}_{(\mathcal{V}, \mathcal{A}) \sim D} [p_F(\mathcal{A}|\mathcal{V}, \mathcal{E}, \mathcal{I}_2)]. \quad (4)$$

### D. Highlight Critical Facial Descriptions as Rationale

In order to obtain the most significant facial expression of the subject for model decision, we prompt the model to answer the instruction  $\mathcal{I}_3$  to highlight, generating a subset of descriptions as rationale  $\mathcal{R}$ . Considering the model may suffer from hallucination, in which unfaithful rationales can degenerate model interpretability and mislead users, we propose a self-refinement based scheme for highlighted rationale.

**Self-refinement for Rationale.** “*Do the highlighted cues really matter to me?*” As the rationales generated by the model itself could be unfaithful due to hallucination [31], we draw inspirations from the work [32] that removes each input feature to measure its attribution, and verify whether the input parts highlighted by the rationale are significant. Since the input instruction contains not only textual descriptions but also visual face images as the original input, it is nontrivial to remove each input part described by the rationale. Here, we propose to identify corresponding regions (e.g., eyebrows, lips, and cheek) in the facial image for each description to be removed, and place mosaic on the exact region of each frame as well. To further verify the faithfulness of the rationale, we remove the facial part reported by the rationale one by one until the model decision is flipped. The least inputs removed that can flip the model decision is recorded as faithfulness score  $f$ . The lower  $f$  is, the more faithful rationale  $R$  is. We thus instruct model  $F$  to reflect on  $R$  and generate  $n$  different rationales, as illustrated in Figure 5. We estimate  $f$  for each rationale,

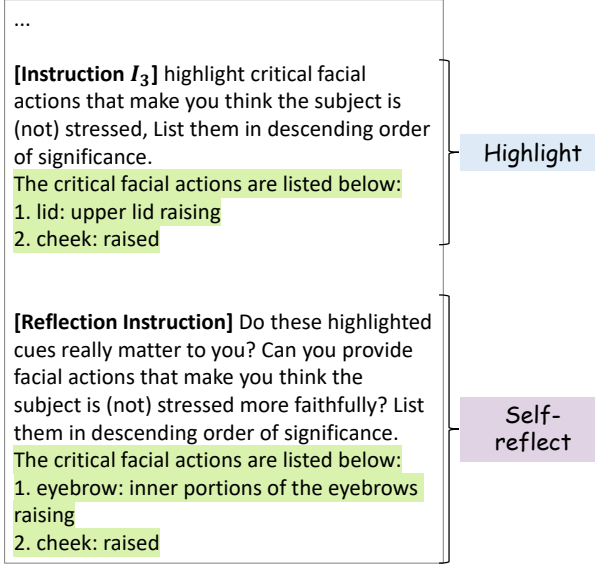


Fig. 5: Illustration of self-reflection process on rationale  $\mathcal{R}$ , where model  $F$  is instructed to reflect on its rationale and generate a new one faithfully.

and select the best rationale  $\mathcal{R}_b$  and the worst rationale  $\mathcal{R}_w$ . We enforce the direct optimization loss to make  $F$  learn to generate faithful rationale as below:

$$\mathcal{L}_{refine\mathcal{R}} = -\mathbb{E}_{\mathcal{V} \sim D} [\log \sigma(\beta \log \frac{p_\theta(\mathcal{R}_b | \mathcal{V}, \mathcal{E}, \mathcal{A}, \mathcal{I}_3)}{p_{ref}(\mathcal{R}_b | \mathcal{V}, \mathcal{E}, \mathcal{A}, \mathcal{I}_3)} - \beta \log \frac{p_\theta(\mathcal{R}_w | \mathcal{V}, \mathcal{E}, \mathcal{A}, \mathcal{I}_3)}{p_{ref}(\mathcal{R}_w | \mathcal{V}, \mathcal{E}, \mathcal{A}, \mathcal{I}_3)})]. \quad (5)$$

The whole learning process of our stress detection model  $F$  is outlined in Algorithm 1.

#### IV. EXPERIMENTS

##### A. Datasets

**Facial Expression Recognition.** To equip the model with the ability to recognize facial actions from videos, we curate a visual instruction tuning dataset from DISFA+ [33], a manually labeled facial expression recognition dataset that contains 645 video samples covering 12 facial action units. Each video sample  $\mathcal{V}$  is annotated with a 12-dimensional label  $a \in \{0, 1\}^{12}$ . We then transform the label into natural linguistic description  $\mathcal{E}$ . For instance, if  $\mathcal{V}$  is annotated with AU 1 (“inner brow raiser”), AU 5 (“upper lid raiser”), and AU 6 (“cheek raiser”), the description  $\mathcal{E}$  is transformed as:

The facial expressions can be listed below:  
-eyebrow: inner portions of the eyebrows raising  
-lid: upper lid raising  
-cheek: raised

**Stress Detection** We consider two video-based stress detection datasets.

(1) The UVSD dataset [10] contains 2092 video samples, featuring 112 college students (58 males and 64 females, aged 18–26). The participants were recorded while watching

##### Algorithm 1: The learning process of model $F$

---

**Input:** Stress detection dataset  $D$  and Facial expression dataset  $D'$ ;  
**Output:** stress detection model  $F$ .  
// Learn to Describe Facial Actions  
1 Train  $F$  with samples from  $D'$  using  $\mathcal{L}_{desc}$  (Eq. 2).  
2 **foreach** sample  $(\mathcal{V}, \mathcal{A})$  from  $D$  **do**  
3     Let  $F$  generate  $\mathcal{E}$  based on  $\mathcal{V}$  and  $\mathcal{I}_1$ .  
        // Update Descriptions  
4     **do**  
5         Let  $F$  reflect on  $\mathcal{E}$  and generate  $\mathcal{E}'$ .  
6         **if**  $h' \geq h$  and  $f' \geq f$  **then**  
7             | Replace  $\mathcal{E}$  with  $\mathcal{E}'$ .  
8         **while**  $f' < f$  or  $h' < h$ ;  
        // Learn to Refine Descriptions  
9         Let  $F$  learns to refine  $\mathcal{E}$  using  $\mathcal{L}_{refine\mathcal{E}}$  (Eq. 3).  
        // Learn to Assess Stress Level  
10         Train  $F$  to generate  $\mathcal{A}$  based on  $\mathcal{V}, \mathcal{E}, \mathcal{I}_2$  using  $\mathcal{L}_{assess}$  (Eq. 4).  
11         Let  $F$  generate  $\mathcal{R}$  based on  $\mathcal{V}, \mathcal{E}, \mathcal{A}, \mathcal{I}_3$ .  
12         Let  $F$  reflect on  $\mathcal{R}$  and generate  $n$  different rationales  $\mathcal{R}'_1, \dots, \mathcal{R}'_n$ .  
13         Evaluate  $\mathcal{R}$  and  $\mathcal{R}'_1, \dots, \mathcal{R}'_n$  to obtain  $\mathcal{R}_b, \mathcal{R}_w$ .  
        // Learn to Refine Rationales  
14         Let  $F$  learns to refine  $\mathcal{R}$  using  $\mathcal{L}_{refine\mathcal{R}}$  (Eq. 5).  
15 **end**

---

videos. The video samples are labeled as “unstressed” when the participants watched content such as scenery, food production, and variety shows. In contrast, they are labeled as “stressed” when the participants watched knowledge-intensive videos and were subsequently given a question-and-answer test. The dataset includes 920 samples labeled as “stressed” and 1,172 labeled as “unstressed”.

(2) The RSL Dataset [34] is curated based on a reality TV program named “Odd Man Out”, in which liars attempted to conceal their identities during conversations and Q&A sessions. It includes a total of 60 subjects with a one-to-one male-to-female ratio. All video frames were refined to depict only one participant per frame, with clear visibility of their face and upper body. 706 video samples were recorded in this dataset, including 209 labeled as “stressed” and 497 labeled as “unstressed”.

##### B. Baseline Methods

**(1) Stress Detection.** We compare the stress detection performance of our method and a few competitive video-based stress detection methods, including 1) Off-the-shelf Large Foundation Models and 2) Supervised Models that learn from annotated datasets.

###### 1) Off-the-shelf Large Foundation Models

**GPT-4o** [35], **Claude-3.5 Sonnet** [36] and **Gemini-1.5 Pro** [37] are three leading state-of-the-art large foundation models with hundreds of billions of parameters and

exhibit impressive vision understanding ability. As they are off-the-shelf and not open sourced, we only use API to let them perform stress detection without training.

## 2) Supervised Models

- **FDASSNN** [38]. It employs an Active Appearance Model (AAM) [39] to detect intensities of different action units, and a multi-layer perceptron to transform action unit intensities into stress detection result.
- **Gao et al.** [12]. It extracts 49 feature points of each face image from a video and apply SVM to classify each frame as positive or negative emotions. When the percentage of frames with negative emotions exceeded a threshold, the video can be classified as stressed.
- **Zhang et al.** [11]. It leverages a Convolutional Neural Network (CNN) to detect emotion in each video frame. If two-thirds of the frames show emotions of anger, sadness, or fear, the video can be detected as having stress.
- **Jeon et al.** [9] It incorporates the features of each video frame encoded by ResNet-18 and the features of facial landmarks encoded by a Facial Landmark Feature Network to form frame-level representations. A temporal attention module further incorporates frame-level representations of each video into stress detection.
- **TSDNet** [10] It first obtains face- and action-level representations separately, and then fuse the results through a stream-weighted integrator with local and global attention for video stress detection.
- **Marlin**. [40] It obtains different face regions and use them to guide the masking autoencoder to generate facial representations.
- **Singh et al.** [41] It detects stress, anxiety and depression from surveillance video samples with ResNet-101 architecture.
- **Ding et al.** [4] It exploits knowledge from large foundation models to describe facial action, and incorporates both facial action descriptions and visual images to detect stress levels.

**(2) Interpretability.** Besides detection performance, we also compare the faithfulness of the rationales generated by our method and three state-of-the-art explainers that require thousands of simulated model results.

- 1) **LIME** [17] is a perturbation-based method that creates visual explanations by randomly masking out portions of an input image to evaluate how these changes influence the model’s predictions.
- 2) **SHAP** [18] uses a game theory to explain the prediction of “black-box” models by constructing an additive feature attribution model that attributes an effect to each input feature, and then summarizing the effects (i.e., Shapley values) as a local approximation of the output.
- 3) **SOBOL** [42] employs Sobol indices to identify the

contribution of the input variables on the variance of the model’s output. It generates a set of real-valued masks using a Quasi-Monte Carlo sequence, which are then applied to an input image to generate the perturbations on the input image.

## C. Performance Metrics

We measure the stress detection performance via Precision, Recall, F1-score, and Accuracy:

- Precision =  $TP / (TP+FN)$ ;
- Recall =  $TP / (TP+TN)$ ;
- F1-score =  $(2 \times \text{Precision} \times \text{Recall}) / (\text{Precision} + \text{Recall})$ ;
- Accuracy =  $(TP+TN) / (TP+TN+FP+FN)$ .

where TP is the true positives, TN is the true negatives, FP is the false positives, and FN is the false negatives. Macro-average is adopted to assign equal weight to each category when calculating the averaged metrics.

We also examine the interpretability of our method, which highlights critical visual cues as the rationale for its stress detection result. We compare the interpretability performance of our method and three computational expensive explainers, by evaluating the drop of model accuracy after disturbing the Top-1, Top-2, and Top-3 scoring segments spotted by each explanation [44].

## D. Main Results

**(1) Performance of Stress Detection.** As shown in Table I, our method outperforms existing approaches on both datasets, achieving the highest accuracy (95.81% on UVSD and 90.94% on RSL) and F1-score (94.22% on UVSD and 85.94% on RSL). It demonstrates significant improvements of 3.33% F1 on UVSD and 5.15% F1 on RSL, compared to the leading supervised baseline proposed by Ding et al. [4]. Moreover, compared to the best-performing large foundation model GPT-4o, our method shows substantial gains of over 17.52% F1 on UVSD and 20.49% F1 on RSL. These results underscore the effectiveness of our method which elucidates the process of reasoning and learns to refine its reasoning in stress detection.

**(2) Performance of Interpretability.** We investigate the interpretability of our method, which highlights critical visual cues as the rationale for its stress detection result, and compare it with those of three other computational expensive explainers. As reported in Table II, our method demonstrates performance on par with the most competitive explainer LIME. The Top-1 accuracy drop of our method significantly outperforms the best-performing baselines with 1.11% on UVSD and 3.09% on RSL. This indicates the Top-1 segment spotted by our method most precisely reflects the model decision.

**(3) Comparison of Computation Efficiency.** We also evaluate the computational efficiency of our method compared to the competing post-hoc explainers. As demonstrated in Figure 6, the average time cost for each testing sample (including describing facial action, assessing stress level, and highlighting the rationale) of our method is 3.4 seconds, which is 63 times faster than the most efficient explainer SOBOL

TABLE I: Stress detection performance of our method and all competitive baselines on the UVSD and RSL dataset, where the best scores are in bold and the second best scores are underlined.

Category	Method	UVSD				RSL			
		Acc.	Prec.	Rec.	F1.	Acc.	Prec.	Rec.	F1.
Large Foundation Models	GPT-4o [43]	75.95%	77.42%	76.93%	76.70%	66.89%	66.01%	68.93%	65.45%
	Claude-3.5 [36]	73.29%	74.11%	73.04%	73.18%	60.76%	61.35%	63.88%	63.42%
Supervised Models	Gemini-1.5 [37]	70.19%	69.91%	72.50%	70.76%	66.53%	65.83%	64.31%	62.07%
	FDASSNN [38]	74.11%	73.71%	74.00%	74.06%	67.42%	62.26%	63.26%	62.75%
Gao et al. [12]	Zhang et al. [11]	78.38%	65.00%	63.83%	64.40%	63.30%	52.81%	62.42%	52.61%
	Jeon et al. [9]	81.58%	67.38%	77.30%	72.00%	65.49%	56.77%	56.21%	56.49%
TSDNet [10]	MARLIN [40]	82.71%	69.61%	77.30%	73.26%	79.53%	74.54%	64.72%	66.78%
	Singh et al. [41]	85.42%	85.28%	85.32%	85.53%	81.76%	80.37%	72.77%	74.99%
Ding et al. [4]	Ding et al. [4]	86.56%	86.56%	87.33%	86.49%	82.50%	84.76%	76.64%	78.64%
	Ours	91.25%	92.18%	90.24%	90.89%	86.50%	84.81%	78.40%	80.79%
		<b>95.81%</b>	<b>96.05%</b>	<b>92.82%</b>	<b>94.22%</b>	<b>90.94%</b>	<b>90.13%</b>	<b>85.13%</b>	<b>85.94%</b>

TABLE II: Accuracy drops after disturbing Top-1, Top-2 and Top-3 scoring segments of the input, where the best scores in bold and the second best scores are underlined.

Method	UVSD			RSL		
	Top-1	Top-2	Top-3	Top-1	Top-2	Top-3
SHAP	8.92%	20.05%	24.49%	9.76%	25.26%	<u>39.81%</u>
LIME	<u>10.85%</u>	<b>28.83%</b>	<b>34.97%</b>	11.54%	<b>30.59%</b>	<b>45.79%</b>
SOBOL	9.14%	19.76%	28.53%	<u>11.61%</u>	25.48%	38.70%
Ours	<b>11.96%</b>	<u>24.31%</u>	<u>29.79%</u>	<b>14.70%</b>	<u>26.70%</u>	35.45%

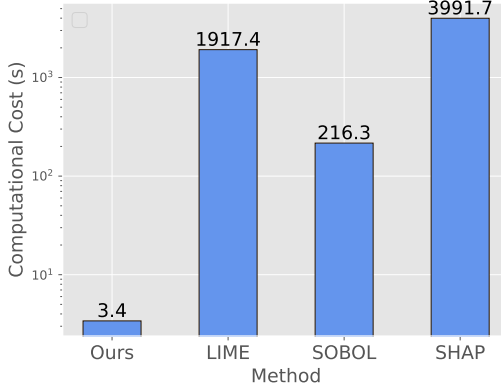


Fig. 6: Comparison of computational costs for explaining a single sample at the testing time.

with 216.3 seconds, proving the benefit of instructing large foundation models to explain themselves.

### E. Ablation Studies

**Impact of Chain Reasoning.** To assess the impact of chain reasoning on stress detection performance, we conduct an ablation study using two ablation variants: “**w/o Chain**”, which directly instructs the model to detect the stress level based on the original video with the prompt “Is the subject in this video stressed? Yes or No?”, and “**w/o learn des.**” which employs the reasoning chain but omits teaching the model how to describe facial actions by removing the loss term in Eq. 2). The results

TABLE III: Performance of our method and ablation variants on chain reasoning.

Dataset	Method	Acc.	Prec.	Rec.	F1.
UVSD	w/o Chain	91.74%	91.97%	90.49%	90.56%
	w/o learn des.	93.75%	93.68%	92.32%	92.64%
	Ours	<b>95.81%</b>	<b>96.05%</b>	<b>92.82%</b>	<b>94.22%</b>
RSL	w/o Chain	86.98%	86.31%	79.96%	80.55%
	w/o learn des.	88.43%	87.27%	83.07%	83.02%
	Ours	<b>90.94%</b>	<b>90.13%</b>	<b>85.13%</b>	<b>85.94%</b>

are presented in Table III, revealing: (1) Omitting the learning of facial action descriptions (“w/o learn des.”) results in a performance drop of 2.06% in accuracy on UVSD and 2.51% on RSL, highlighting the importance of facial action knowledge in guiding the model to focus on key facial expressions for stress detection. (2) Excluding the chain reasoning process entirely (“w/o Chain”) leads to a more substantial performance decline, with accuracy reductions of 4.07% on UVSD and 3.96% on RSL. These findings underscore the significant contribution of incorporating a step-by-step reasoning process to enhance detection performance.

We also compare the interpretability performance of our model with its variants “**w/o Chain**” and “**w/o learn des.**”. Note that “**w/o Chain**” guides the model to assess the stress level with instruction  $\mathcal{I}_2$ , and then guides the model to highlight key facial actions with  $\mathcal{I}_3$ . As shown in Table IV, removing chain reasoning leads to performance decline of 5.67% on UVSD and 7.54% on RSL, when the Top-1 scoring segment is disturbed from the input. This suggests that the reasoning process (i.e., systematically describing all facial actions present in the video) helps the model identify critical facial actions. Additionally, the Top-1 performance of the model decreases by 1.04% on UVSD and 2.23% on RSL, further demonstrating the importance of facial action knowledge in finalizing the rationale for predictions.

**Impact of Self-refine Learning Scheme.** To investigate the effectiveness of the self-refine learning scheme, we design the following ablation variants: “**w/o refinement**” removes the

TABLE IV: Accuracy drop for our rationale and ablation variants on chain reasoning.

Method	UVSD			RSL		
	Top-1	Top-2	Top-3	Top-1	Top-2	Top-3
w/o Chain	6.29%	14.98%	20.05%	7.16%	18.86%	27.64%
w/o learn des.	10.92%	18.46%	24.39%	12.47%	24.20%	33.36%
Ours	<b>11.96%</b>	<b>24.31%</b>	<b>29.79%</b>	<b>14.70%</b>	<b>29.52%</b>	<b>38.06%</b>

TABLE V: Performance of our method and ablation variants on Self-refine learning.

Dataset	Method	Acc.	Prec.	Rec.	F1.
UVSD	w/o Refine	93.56%	94.33%	91.10%	92.68%
	w/o Reflection	94.99%	95.27%	92.05%	93.36%
	Ours	<b>95.81%</b>	<b>96.05%</b>	<b>92.82%</b>	<b>94.22%</b>
RSL	w/o Refine	88.79%	89.12%	83.24%	84.01%
	w/o Reflection	89.71%	89.58%	84.75%	85.36%
	Ours	<b>90.94%</b>	<b>90.13%</b>	<b>85.13%</b>	<b>85.94%</b>

entire self-refine learning scheme; “**w/o reflection**” removes the self-reflection process that guides the model to generate different descriptions (Fig. 3) and rationales (Fig. 5). Instead, this variant simply samples different descriptions and rationales from the model using instructions  $\mathcal{I}_1$  and  $\mathcal{I}_3$ . The results, presented in Table V, reveal the following: (1) The self-refinement learning scheme improves detection accuracy by 2.25% on UVSD and 2.15% on RSL, demonstrating the model’s ability to enhance its reasoning chain by learning from its outputs. (2) Removing the self-reflection process (“**w/o reflection**”) results in accuracy declines of 0.82% on UVSD and 1.23% on RSL, further highlighting the effectiveness of self-reflection in eliciting more valuable generations (e.g., facial descriptions) compared to repeated sampling.

We also compare the interpretability performance of our model against the ablation variants “**w/o refinement**” and “**w/o reflection**”. Table VI shows that excluding self-refine learning leads to Top-1 performance drop of 3.07% on UVSD and 2.89% on RSL. This verifies the model itself can perform additional refinement targeting at providing more faithful intermediate results (i.e., facial action descriptions) and final rationale (i.e., highlighted facial actions). Additionally, removing the self-reflection process results in Top-1 performance drop of 0.82% on UVSD and 0.85% on RSL, showcasing self-reflection as an effective strategy in eliciting more faithful results from the model.

#### F. Further Analysis of Impact of In-context Examples

Large foundation models have demonstrated strong in-context learning abilities, enabling them to learn from examples provided in the context before answering task-specific questions. Notably, prior studies have shown that in-context examples with semantics similar to the query can significantly enhance the performance [45]. In this study, we investigate the performance of our method when using in-context examples retrieved from the training dataset. To explore this, we apply different retrieval

TABLE VI: Accuracy drop for our rationale and ablation variants on chain reasoning.

Method	UVSD			RSL		
	Top-1	Top-2	Top-3	Top-1	Top-2	Top-3
w/o Refine	8.89%	21.43%	25.98%	11.81%	24.79%	32.12%
w/o Reflection	11.14%	19.75%	24.91%	13.85%	27.80%	35.96%
Ours	<b>11.96%</b>	<b>24.31%</b>	<b>29.79%</b>	<b>14.70%</b>	<b>29.52%</b>	<b>38.06%</b>

TABLE VII: Performance comparison of different methods in retrieving in-context examples.

Dataset	Method	Acc.	Prec.	Rec.	F1.
UVSD	w/o example	95.81%	96.05%	92.82%	94.22%
	Random	95.43%	95.87%	93.01%	93.98%
	Retrieve-by-vision	96.25%	96.43%	94.65%	94.32%
	Retrieve-by-description	<b>96.79%</b>	<b>97.03%</b>	<b>95.36%</b>	<b>95.16%</b>
RSL	w/o Example	90.94%	90.13%	85.13%	85.94%
	Random	90.69%	90.44%	85.40%	85.86%
	Retrieve-by-vision	92.71%	91.92%	87.40%	89.19%
	Retrieve-by-description	<b>94.05%</b>	<b>92.72%</b>	<b>88.37%</b>	<b>90.20%</b>

methods for selecting in-context examples for each testing sample: for each testing sample, (1) “**Random**” randomly assigns a training sample as the in-context example; (2) “**Retrieve-by-vision**” extracts visual semantics from the video sample with a Videoformer [46] encoder, and then selects the most similar example to the testing sample using cosine similarity metric [47]; (3) “**Retrieve-by-description**” employs a BERT encoder [48] to transform the facial action description of each sample into a textual representation. After the model generating facial action descriptions for a testing sample, it selects the training sample with the closest cosine similarity of textual representation. From the performance results presented in Table VII, we can observe that (1) both “**Retrieve-by-vision**” and “**Retrieve-by-description**” improve the detection accuracy by at least 0.44% on UVSD and 1.77% on RSL, demonstrating that retrieving semantically similar examples helps inspire the model. This suggests that the training dataset not only supports fine-tuning but also serves as a valuable resource for knowledge sharing. (2) Despite the improvement brought by “**Retrieve-by-vision**” and “**Retrieve-by-description**”, the performance of randomly selecting examples (“**Random**”) cannot surpass removing in-context examples (“**w/o Example**”). This further indicates the model benefits from knowledge and experience from samples of similar semantics. (3) Compared with “**Retrieve-by-vision**”, “**Retrieve-by-description**” demonstrates better performance with 0.54% of accuracy improvement on UVSD and 1.34% on RSL. It indicates the model itself could be a better selector: its descriptions can better help retrieve similar samples to answer the testing sample. This assumption is also evidenced in Figure 7, in which we compute the cosine similarities between one testing sample and training samples. The training samples are categorized into “**Helpful**” samples, which could help the model generate the correct stress result, as well as “**Unhelpful**” samples, which could lead to incorrect results. Compared with

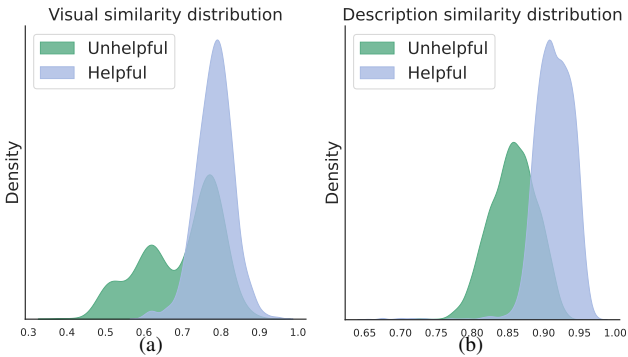


Fig. 7: (a) Similarities between the visual representations of the testing sample and training samples; (b) Similarities between the descriptions of the testing sample and training samples.

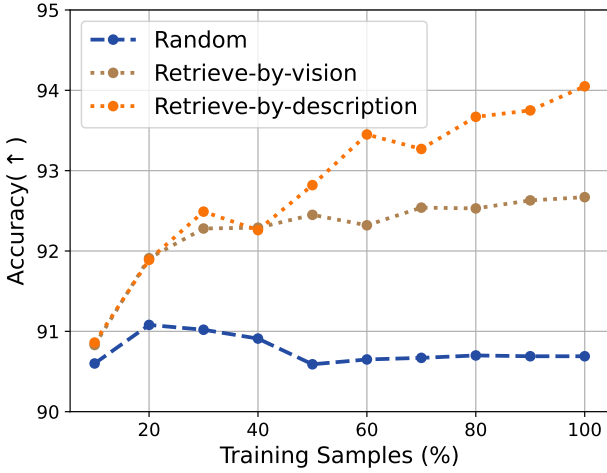


Fig. 8: Effect of training sample sizes for in-context example retrieval.

Figure 7(a), which uses visual representations encoded by Videoformer (“retrieve-by-vision”), Figure 7(b) makes it easier to distinguish “Helpful” samples from “Unhelpful” ones with textual representations encoded from descriptions (“retrieve-by-description”).

Furthermore, we investigate the effect of varying training sample sizes for in-context example selection. Specifically, we extract each subset from the original training dataset of RSL, and evaluate the performance with each retrieval method. Figure 8 shows the effect of different sizes of training samples in RSL for retrieval. We can observe that the model benefits from a larger resource of samples if we retrieve similar ones as in-context examples. Therefore, more efficient data management and retrieval techniques could be further explored to support large-scale in-context example resource.

#### G. Generalizing to the Off-the-Shelf Large Foundation Models

To evaluate the generalization ability of our method, we apply our chain reasoning scheme to three off-the-shelf large foundation models for stress detection. Concretely, we instruct them to describe the facial actions with instruction  $\mathcal{I}_1$  first,

TABLE VIII: Performance of the off-the-shelf large foundation models after applying our method.

Dataset	Method		Acc.	Prec.	Rec.	F1.
UVSD	GPT-4o	Original	75.95%	77.42%	76.93%	76.70%
		New	<b>81.49%</b>	<b>81.12%</b>	<b>79.36%</b>	<b>79.97%</b>
RSL	Claude-3.5	Original	73.29%	74.11%	73.04%	73.18%
		New	<b>75.89%</b>	<b>74.32%</b>	<b>75.01%</b>	<b>74.25%</b>
Gemini-1.5	GPT-4o	Original	70.19%	69.91%	72.50%	70.76%
		New	<b>73.43%</b>	<b>72.78%</b>	<b>74.91%</b>	<b>71.80%</b>
GPT-4o	Claude-3.5	Original	66.89%	66.01%	68.93%	65.45%
		New	<b>74.06%</b>	<b>72.73%</b>	<b>70.55%</b>	<b>70.16%</b>
Gemini-1.5	Claude-3.5	Original	60.76%	61.35%	63.88%	63.42%
		New	<b>63.50%</b>	<b>65.53%</b>	<b>68.48%</b>	<b>67.11%</b>
Gemini-1.5	GPT-4o	Original	66.53%	65.83%	64.31%	62.07%
		New	<b>70.34%</b>	<b>68.31%</b>	<b>68.10%</b>	<b>66.73%</b>

followed by guiding them to assess the stress level using  $\mathcal{I}_2$ . Since fine-tuning the model parameters during the training phase is not possible, we employ self-refinement at the testing phase instead. We instruct the model to reflect on its initial descriptions  $\mathcal{E}$ , and generate a different set of descriptions following Figure 3. We only compare the faithfulness of each set of descriptions, by starting another conversation session of the model to verify whether the new set of descriptions more honestly describes the original video (Fig. 4). The model is prompted to reassess the stress level only if it cannot produce a more faithful set of descriptions. We evaluate the performance of three off-the-shelf large foundation models after applying our method. Table VIII shows our method enhances the detection accuracy of three off-the-shelf models by at least 2.60% on UVSD and 2.74% on RSL. Notably, GPT-4o improves by 5.54% on UVSD and 7.17% on RSL, demonstrating the generalization ability of our method.

#### H. Experimental Details

We use Qwen-VL [49] to initialize our model (7 billion parameters). To fine-tune our model, we set the learning rate to 1e-4, number of training epochs to 10, and the batch size to 32. For DPO optimization, we set hyper-parameter  $\beta$  to 0.1. All experiments are performed on 2 V100 GPUs (32GB). For all experiments, we perform 10-fold cross validation, and report the average score of each method. The original format of image frames from UVSD and RSL dataset is  $640 \times 480$  ( $height \times width$ ), we resize the original video frames into  $96 \times 96$ . To minimize the computation cost, from each original video sample we extract the frame with the most expressive face  $f_e$ , and the frame with the least expressive face  $f_l$  following Zhang et al. [10], and feed them into the model as input  $\mathcal{V}$ . To evaluate the interpretability performance of our framework and baselines, we employ the SLIC algorithm to segment  $f_e$  into 64 segments, and place gaussian noise on the top scoring segments highlighted by each method [44]. For our framework, after generating highlighted rationale  $\mathcal{R}$ , we locate the segment of each single facial action using the corresponding facial

landmark. For LIME and SHAP, the number of evaluations for each sample is set to 1000.

## V. CONCLUSION

We introduce a novel approach to video-based stress detection which transforms the detection process into an expert-like “*Describe*→*Assess*→*Highlight*” reasoning chain, and learns to refine its reasoning during the training process. As the outcome, the method not only predicts stress levels but also provides interpretable rationales efficiently. Our extensive experiments demonstrate that our method outperforms state-of-the-art methods in both accuracy and interpretability across two distinct datasets.

## REFERENCES

- [1] A. Tiwari, B. Matejek, and D. Haehn, “Non-invasive stress monitoring from video,” in *2024 IEEE International Symposium on Biomedical Imaging (ISBI)*. IEEE, 2024, pp. 1–5.
- [2] A. R. Javed, W. Ahmed, S. Pandya, P. K. R. Maddikunta, M. Alazab, and T. R. Gadekallu, “A survey of explainable artificial intelligence for smart cities,” *Electronics*, vol. 12, no. 4, p. 1020, 2023.
- [3] C. Molnar, *Interpretable machine learning*. Lulu. com, 2020.
- [4] Y. Ding, Y. Dai, X. Wang, L. Feng, L. Cao, and H. Zhang, “Integrating content-semantics-world knowledge to detect stress from videos,” in *ACM Multimedia 2024*.
- [5] J. Wei, X. Wang, D. Schuurmans, M. Bosma, F. Xia, E. Chi, Q. V. Le, D. Zhou *et al.*, “Chain-of-thought prompting elicits reasoning in large language models,” *Advances in neural information processing systems*, vol. 35, pp. 24 824–24 837, 2022.
- [6] W.-J. Yan, X. Li, S.-J. Wang, G. Zhao, Y.-J. Liu, Y.-H. Chen, and X. Fu, “Casme ii: An improved spontaneous micro-expression database and the baseline evaluation,” *PloS one*, vol. 9, no. 1, p. e86041, 2014.
- [7] E. Yee, A. Li, C. Tang, Y. H. Jung, R. Paturi, and L. Bergen, “Faithful and unfaithful error recovery in chain of thought,” in *First Conference on Language Modeling*, 2024. [Online]. Available: <https://openreview.net/forum?id=IPZ28ZqD4I>
- [8] R. Rafailov, A. Sharma, E. Mitchell, C. D. Manning, S. Ermon, and C. Finn, “Direct preference optimization: Your language model is secretly a reward model,” *Advances in Neural Information Processing Systems*, vol. 36, 2024.
- [9] T. Jeon, H. B. Bae, Y. Lee, S. Jang, and S. Lee, “Deep-learning-based stress recognition with spatial-temporal facial information,” *Sensors*, vol. 21, no. 22, p. 7498, 2021.
- [10] H. Zhang, L. Feng, N. Li, Z. Jin, and L. Cao, “Video-based stress detection through deep learning,” *Sensors*, vol. 20, no. 19, p. 5552, 2020.
- [11] J. Zhang, X. Mei, H. Liu, S. Yuan, and T. Qian, “Detecting negative emotional stress based on facial expression in real time,” in *2019 IEEE 4th Int'l Conf. on signal and image processing (ICSIP)*. IEEE, 2019, pp. 430–434.
- [12] H. Gao, A. Yüce, and J.-P. Thiran, “Detecting emotional stress from facial expressions for driving safety,” in *2014 IEEE Int'l Conf. on Image Processing (ICIP)*. IEEE, 2014, pp. 5961–5965.
- [13] J. F. Cohn, Z. Ambadar, and P. Ekman, “Observer-based measurement of facial expression with the facial action coding system,” *The handbook of emotion elicitation and assessment*, vol. 1, no. 3, pp. 203–221, 2007.
- [14] C. Viegas, S.-H. Lau, R. Maxion, and A. Hauptmann, “Towards independent stress detection: A dependent model using facial action units,” in *2018 Int'l Conf. on content-based multimedia indexing (CBMI)*. IEEE, 2018, pp. 1–6.
- [15] G. Giannakakis, M. R. Koujan, A. Roussos, and K. Marias, “Automatic stress detection evaluating models of facial action units,” in *2020 15th IEEE international conference on automatic face and gesture recognition (FG 2020)*. IEEE, 2020, pp. 728–733.
- [16] R. Benassi, F. Guerra, M. Paganelli, and D. Tiano, “Explaining entity matching with clusters of words,” in *2024 IEEE 40th International Conference on Data Engineering (ICDE)*. IEEE, 2024, pp. 2325–2337.
- [17] M. T. Ribeiro, S. Singh, and C. Guestrin, ““ why should i trust you?” explaining the predictions of any classifier,” in *Proceedings of the 22nd ACM SIGKDD international conference on knowledge discovery and data mining*, 2016, pp. 1135–1144.
- [18] S. Lundberg, “A unified approach to interpreting model predictions,” *arXiv preprint arXiv:1705.07874*, 2017.
- [19] S. Huang, S. Mamidanna, S. Jangam, Y. Zhou, and L. H. Gilpin, “Can large language models explain themselves? a study of llm-generated self-explanations,” *arXiv preprint arXiv:2310.11207*, 2023.
- [20] T. Kojima, S. S. Gu, M. Reid, Y. Matsuo, and Y. Iwasawa, “Large language models are zero-shot reasoners,” *Advances in neural information processing systems*, vol. 35, pp. 22 199–22 213, 2022.
- [21] L. Gao, A. Madaan, S. Zhou, U. Alon, P. Liu, Y. Yang, J. Callan, and G. Neubig, “Pal: Program-aided language models,” in *International Conference on Machine Learning*. PMLR, 2023, pp. 10 764–10 799.
- [22] X. Li and X. Qiu, “Mot: Memory-of-thought enables chatgpt to self-improve,” *arXiv preprint arXiv:2305.05181*, 2023.
- [23] K. Shum, S. Diao, and T. Zhang, “Automatic prompt augmentation and selection with chain-of-thought from labeled data,” *arXiv preprint arXiv:2302.12822*, 2023.
- [24] S. Pitis, M. R. Zhang, A. Wang, and J. Ba, “Boosted prompt ensembles for large language models,” *arXiv preprint arXiv:2304.05970*, 2023.
- [25] H. Chae, Y. Song, K. T. Ong, T. Kwon, M. Kim, Y. Yu, D. Lee, D. Kang, and J. Yeo, “Dialogue chain-of-thought distillation for commonsense-aware conversational agents,” in *Proceedings of the 2023 Conference on Empirical*

*Methods in Natural Language Processing, EMNLP 2023, Singapore, December 6-10, 2023*, H. Bouamor, J. Pino, and K. Bali, Eds. Association for Computational Linguistics, 2023, pp. 5606–5632. [Online]. Available: <https://doi.org/10.18653/v1/2023.emnlp-main.342>

[26] O. Gramopadhye, S. S. Nachane, P. Chanda, G. Ramakrishnan, K. S. Jadhav, Y. Nandwani, D. Raghu, and S. Joshi, “Few shot chain-of-thought driven reasoning to prompt llms for open ended medical question answering,” *arXiv preprint arXiv:2403.04890*, 2024.

[27] V. Liévin, C. E. Hother, A. G. Motzfeldt, and O. Winther, “Can large language models reason about medical questions?” *Patterns*, vol. 5, no. 3, 2024.

[28] J. Lee, L. H. Pham, and Ö. Uzuner, “Enhancing consumer health question reformulation: Chain-of-thought prompting integrating focus, type, and user knowledge level,” in *Proceedings of the First Workshop on Patient-Oriented Language Processing (CL4Health) @ LREC-COLING 2024*, D. Demner-Fushman, S. Ananiadou, P. Thompson, and B. Ondov, Eds. Torino, Italia: ELRA and ICCL, May 2024, pp. 220–228. [Online]. Available: <https://aclanthology.org/2024.cl4health-1.27>

[29] Q. Lyu, S. Havaldar, A. Stein, L. Zhang, D. Rao, E. Wong, M. Apidianaki, and C. Callison-Burch, “Faithful chain-of-thought reasoning,” *arXiv preprint arXiv:2301.13379*, 2023.

[30] S. H. Lee and Y. M. Ro, “Partial matching of facial expression sequence using over-complete transition dictionary for emotion recognition,” *IEEE Transactions on Affective Computing*, vol. 7, no. 4, pp. 389–408, 2015.

[31] Y. Zhang, Y. Li, L. Cui, D. Cai, L. Liu, T. Fu, X. Huang, E. Zhao, Y. Zhang, Y. Chen *et al.*, “Siren’s song in the ai ocean: a survey on hallucination in large language models,” *arXiv preprint arXiv:2309.01219*, 2023.

[32] C. Agarwal and A. Nguyen, “Explaining image classifiers by removing input features using generative models,” in *Proceedings of the Asian Conference on Computer Vision*, 2020.

[33] M. Mavadati, P. Sanger, and M. H. Mahoor, “Extended disfa dataset: Investigating posed and spontaneous facial expressions,” in *2016 IEEE Conference on Computer Vision and Pattern Recognition Workshops (CVPRW)*, 2016, pp. 1452–1459.

[34] B. M. DePaulo, J. J. Lindsay, B. E. Malone, L. Muhlenbruck, K. Charlton, and H. Cooper, “Cues to deception.” *Psychological bulletin*, vol. 129, no. 1, p. 74, 2003.

[35] Openai, “<https://openai.com/index/hello-gpt-4o/>,” 2024.

[36] Anthropic, “Claude 3.5 sonnet,” <https://www.anthropic.com/news/clause-3-5-sonnet>, 2024.

[37] G. Team, P. Georgiev, V. I. Lei *et al.*, “Gemini 1.5: Unlocking multimodal understanding across millions of tokens of context,” 2024. [Online]. Available: <https://arxiv.org/abs/2403.05530>

[38] M. Gavrilescu and N. Vizireanu, “Predicting depression, anxiety, and stress levels from videos using the facial action coding system,” *Sensors*, vol. 19, no. 17, p. 3693, 2019.

[39] G. J. Edwards, C. J. Taylor, and T. F. Cootes, “Interpreting face images using active appearance models,” in *Proceedings Third IEEE Int’l Conf. on Automatic Face and Gesture Recognition*. IEEE, 1998, pp. 300–305.

[40] Z. Cai *et al.*, “Marlin: Masked autoencoder for facial video representation learning,” in *CVPR*, 2023, pp. 1493–1504.

[41] A. Singh *et al.*, “Detection of stress, anxiety and depression (sad) in video surveillance using resnet-101,” *Microprocessors and Microsystems*, vol. 95, 2022.

[42] T. Fel, R. Cadene, M. Chalvidal, M. Cord, D. Vigouroux, and T. Serre, “Look at the variance! efficient black-box explanations with sobol-based sensitivity analysis,” in *Advances in Neural Information Processing Systems (NeurIPS)*, 2021.

[43] J. Achiam, S. Adler, S. Agarwal, L. Ahmad, I. Akkaya, F. L. Aleman, D. Almeida, J. Altenschmidt, S. Altman, S. Anadkat *et al.*, “Gpt-4 technical report,” *arXiv preprint arXiv:2303.08774*, 2023.

[44] K. Tsigos, E. Apostolidis, S. Baxevanakis, S. Papadopoulos, and V. Mezaris, “Towards quantitative evaluation of explainable ai methods for deepfake detection,” in *Proceedings of the 3rd ACM International Workshop on Multimedia AI against Disinformation*, 2024, pp. 37–45.

[45] Y. Zhang, K. Zhou, and Z. Liu, “What makes good examples for visual in-context learning?” in *Advances in Neural Information Processing Systems*, A. Oh, T. Naumann, A. Globerson, K. Saenko, M. Hardt, and S. Levine, Eds., vol. 36. Curran Associates, Inc., 2023, pp. 17 773–17 794. [Online]. Available: [https://proceedings.neurips.cc/paper\\_files/paper/2023/file/398ae57ed4fda79d0781c65c926d667b-Paper-Conference.pdf](https://proceedings.neurips.cc/paper_files/paper/2023/file/398ae57ed4fda79d0781c65c926d667b-Paper-Conference.pdf)

[46] Y. Ge, Y. Ge, X. Liu, D. Li, Y. Shan, X. Qie, and P. Luo, “Bridgeformer: Bridging video-text retrieval with multiple choice questions,” *arXiv preprint arXiv:2201.04850*, 2022.

[47] S. H. Lee, J. Ke, Y. Li, J. He, S. Hickson, K. Datsenko, S. Kim, M.-H. Yang, I. Essa, and F. Yang, “Cropper: Vision-language model for image cropping through in-context learning,” 2024. [Online]. Available: <https://arxiv.org/abs/2408.07790>

[48] J. Devlin, M.-W. Chang, K. Lee, and K. Toutanova, “Bert: Pre-training of deep bidirectional transformers for language understanding,” *arXiv preprint arXiv:1810.04805*, 2018.

[49] J. Bai, S. Bai, S. Yang, S. Wang, S. Tan, P. Wang, J. Lin, C. Zhou, and J. Zhou, “Qwen-vl: A versatile vision-language model for understanding, localization, text reading, and beyond,” 2023. [Online]. Available: <https://arxiv.org/abs/2308.12966>